university of groningen

faculty of science and engineering

Characterization and optimization of CsI and NaI(Tl) detectors for GAINS

Geet Kalsulkar

university of groningen

faculty of science and engineering

University of Groningen

Characterization and optimization of CsI and NaI(Tl) detectors for GAINS

Master's Thesis

To fulfill the requirements for the degree of
Master of Science in Physics (track: *Quantum Universe*)
at University of Groningen under the supervision of
Prof. dr. Myroslav Kavatsyuk
and
Prof. dr. N. Kalantar-Nayestanaki

Geet Kalsulkar

2nd June 2023

Contents

List of abbreviations

ADC: Analog to digital converter

CsI: Caesium iodide

GAINS: Gamma Array for Inelastic Neutron Scattering

MSR: Molten salt reactor

GEANT4: **GE**ometry **AN**d **T**racking

GELINA: Geel Electron Linear Accelerator

GUI: Graphical user interface

HPGe: High purity Germanium

NaI: Sodium iodide

ZnS: Zinc sulphide

Abstract

The GAINS spetrometer at GELINA facility was developed to study inelastic neutron scattering cross sections to help develop a new generation of nuclear reactors. The GAINS spectrometer consists of twelve HPGe detectors in a rear-hemispherical configuration [1]. HPGe detectors have excellent energy resolution. The use of HPGe detectors pose certain issues like high operational costs and small crystal size i.e. less coverage area.

In this research four CsI and one NaI(Tl) scintillation detectors were characterized and optimized. Emphasis was given on optimizing individual detector parameters to obtain best energy resolution. Data acquisition was done using ^{60}Co and ^{22}Na as gamma sources. Obtained experimental data and data procured from GAINS experiments was used to develop Monte Carlo simulations. The data acquired from these simulations of GAINS spectrometer along with NaI and CsI based GAINS-like setups was compared. The viability of the CsI and NaI(Tl) detectors to be used in a similar configuration to GAINS was investigated. Results presented in this thesis are based on energy dependent characteristics of HPGe, NaI(Tl) and CsI based detection setups.

1 Introduction

Gamma spectrometry using scintillation detectors is an important research field. Its applications can be seen in diverse fields like nuclear and high energy physics, medical imaging and so on. Scintillators (solid, liquid or gas) are materials that exhibit luminescence when ionizing radiation passes through them [2]. The luminescence produced in scintillators is too small to be measured directly. Hence, these crystals are coupled with photomultiplier tubes (PMTs). PMTs as the name suggests are amplifiers for photons. A scintillation crystal coupled with PMT is a radiation detector. Based on the material, the scintillators are characterized into three groups; inorganic, organic and gaseous scintillators.

Most of inorganic scintillators are crystals of alkali metals, in particular alkali iodides, that contain a small percentage of impurity. This research deals with optimization and characterization of CsI and NaI(Tl) detectors. These detectors are investigated in order to develop a radiation detection array similar to GAINS at GELINA.

1.1 GAINS at GELINA

Gamma Array for Inelastic Neutron Scattering (GAINS) is a spectrometer setup consisting of twelve HPGe detectors. It is located at the Geel Electron Linear Accelerator (GELINA) in Belgium. Measurement of neutron cross-sections with high precision is an important aspect of research in nuclear energy. The GAINS spectrometer at GELINA was developed to study the various neutron interactions and cross sections to help further the research into generation four molten salt reactors (MSRs).

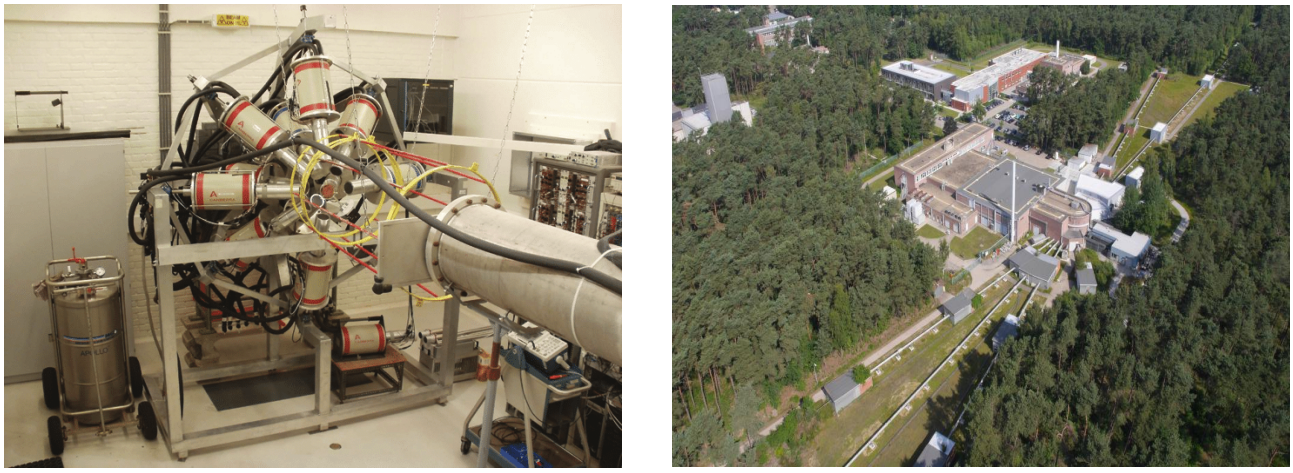

Figure 1: (*left*) GAINS spectrometer at GELINA . (*right*) Aerial view of GELINA facility.

GELINA is a neutron time of flight (nTOF) facility with several flight paths with varying lengths (10 m - 400 m). The linear accelerator (LINAC) is used to generate an electron beam which is time compressed using magnets to get a small pulse width (typically 1 ns). This is then sent on to a uranium (U) target where neutrons are produced via (γ , n) and (γ , f) reactions. The generated neutrons are then scattered using any target of interest. The scattering of neutrons produces gamma radiation which is recorded using the GAINS spectrometer. GAINS consists of twelve HPGe detectors at 100% relative efficiency. The detectors are placed in rear hemisphere configuration with angles 110°, 125°and 150° [3].

1.2 Research Overview

The aim of this research is to study the behavior of CsI and NaI(Tl) detectors so as to determine the feasibility of these detectors to be used in a similar configuration as the GAINS setup. This is to be done in order to expand the scope of measurements to be performed at GELINA facility.

Before setting up the CsI and NaI(Tl) detectors in actual GAINS-like configuration and testing them, we need to determine the feasibility of individual detectors. The detectors available were discarded from front line research because of their age. Hence, testing each detector prior to proceeding with experiments takes precedence. Therefore, this research is divided into three phases.

1. Detector optimization

This phase includes testing the individual detectors. The goal of this phase is to determine the optimal experimental parameters for individual detectors. This is done with one NaI(Tl) and four CsI detectors. To analyse the behavior and determine the optimal parameters, a 16 channel SIS3316 VME digitizer manufactured by Struck was used in conjunction with an oscilloscope.

2. Methods and measurement

The second phase deals with data acquisition and the analysis of the data acquired from each detector set at optimal parameters with radioactive sources. Each detector was tested with ^{60}Co, ^{22}Na, ^{241}Am radioactive sources. However, the ^{241}Am was later discarded as the γ peak was unresolved due to high background noise.

3. Simulation environment

This phase which encompasses the development of a simulation of the experimental setup (individual detectors) using GEANT4 [4]. The simulation is done to replicate the experiments in phase two but this time using GEANT4 simulation software. The data acquired through these simulations is then compared with the experimental data to check the simulation viability. Then the simulation is expanded to a twelve detector setup; for CsI and NaI(Tl) respectively; which is similar to the GAINS configuration. Then data acquisition is performed using the simulated GAINS configuration with CsI and NaI(Tl) detectors.

The data acquired from these simulation holds the key to understanding the feasibility of GAINS-like setup with CsI or NaI(Tl) detectors. Also it helps to determine the operational energies and energy resolution of such a setup. This would help in determining the experimental scope of such a setup.

2 Detector optimization

To get an idea about why this research is done the way it is, first we need to refresh our understanding regarding scintillation detectors. In 1903, William Crookes was the first to observe this scintillation phenomenon with α particles impinging on ZnS screen [2]. The amount of light emitted by this phenomenon is very small. Although this phenomenon was discovered in 1903, it took many years of technological development in electronics to be able to refine this phenomenon into a viable radiation detection technique.

2.1 Scintillator principles

Scintillators (solid, liquid or gas) are materials that exhibit luminescence when ionizing radiation passes through them. This research deals with inorganic scintillation detectors of flavours CsI and NaI(Tl). In both the cases the mechanism of a scintillation detector can be described broadly in two stages. The first stage is the excitation of the electrons in crystal by absorption of incident radiation by the scintillator, followed by production of photons during the de-excitation. This is then followed by the amplification of the current generated by the photons in the photomultiplier tube. This amplified electrical pulse is delivered as the output signal. A scintillation detector is thus a scintillating material optically coupled with a photomultiplier tube (PMT). The output pulse, depending on the nature of the detector is either amplified again by an external amplifier or used as is for further analysis based on the demands of the experiment.

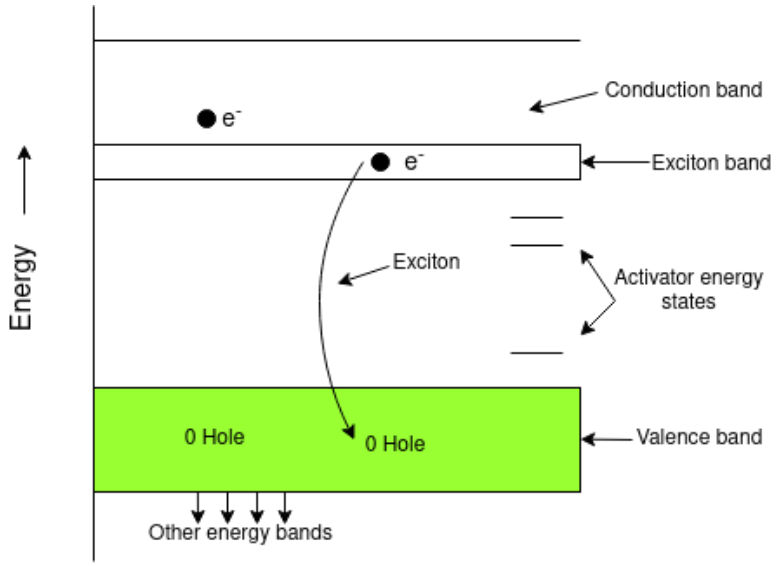

Figure 2: Energy band schematic of a crystal.

The mechanism of scintillation process in inorganic crystals depends on the electronic energy states of the crystal lattice. In a crystal the discrete energy levels broaden into bands. The lower energy band, also known as *valence* band represents the electrons bound at the lattice sites. The higher energy band known as *conduction* band represents electrons which are free to migrate in the lattice. Note that the conduction band is empty in the ground state. When the incident radiation is insufficient to excite the electron to the conduction band, an electron-hole bound pair (also known as *exciton*) is formed.

The exciton energy states form a thin energy band whose upper level coincides with the lower level of the conduction band [2]. In case of pure crystals the de-excitation of electron into valence band is an inefficient process. Typically the band gaps are such that the emitted photon has too much energy to be in the visible spectrum. To increase the chance of visible photon emission, small amounts of impurities are added while growing the scintillation crystal. These impurities also known as *activators* modify the energy band structure at their sites in the lattice. This results in the creation of energy states in the forbidden band of the pure crystal. The de-excitation process thus takes place via these activator energy states. These sites in the lattice are known as *luminescence centres* [5]. As the energy during de-excitation is less than the full forbidden band, the transition gives rise to visible photon. The CsI detectors used in this research do not have any added impurities i.e. they are pure CsI crystal detectors. This implies that the light yield from these detectors is low compared to doped CsI(Tl) or CsI(Na) based detectors. However, the NaI(Tl) detector used in this research has thallium as the doped impurity in the crystal which implies comparatively higher light yeild.

(a) CsI detector (b) NaI(Tl) detector

Figure 3: Detectors with shielding removed.

2.2 Experimental setup

As mentioned previously, the first order of business is to test all the detectors individually. This includes optimization of the experimental parameters. However, before moving to the parameters we need to setup the necessary equipment to start testing the detectors. The equipment required for the experiments consists of a high voltage (HV) source capable of providing both positive and negative voltages (CsI detector requires negative voltage whereas NaI(Tl) requires positive voltage), a timing and filter amplifier, oscilloscope and a Struck SIS3316 digitizer connected to a computer, etc.

The schematic of a scintillation detector setup is shown in figure 4. In this case, detector is connected to the high voltage source. The signals from all the detectors were first examined using an oscilloscope. Then depending on the amplitude of the output pulse, it is to be determined if it should be amplified before passing it to the SIS3316 digitizer. This is because the SIS3316 has two input bands of 2.5 V and 5 V maximum. These bands refer to the input signal amplitude which can be passed through the digitizer to obtain best results from the output of a detector. Along with amplitude, the

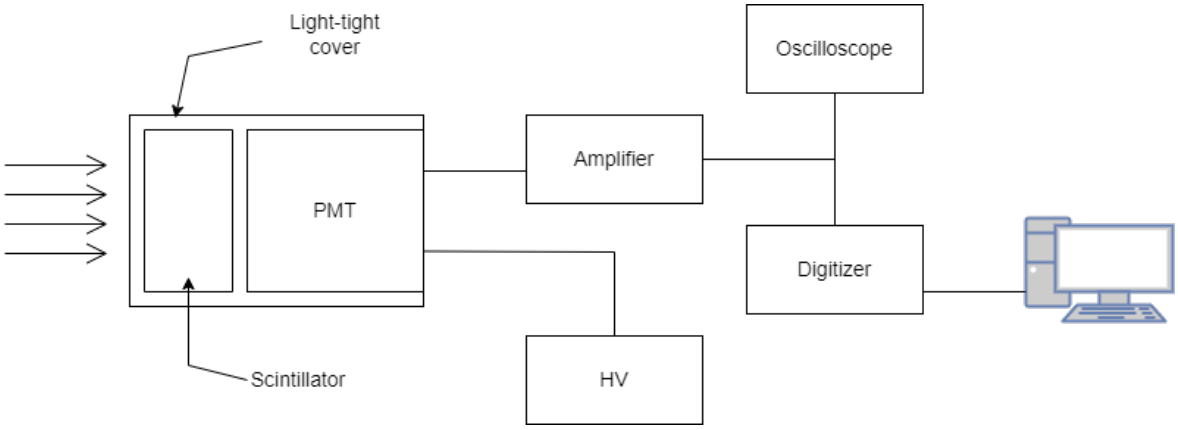

Figure 4: Generalized detector system using a scintillator.

pulse width needs to be sufficiently large as to not cause an overlap within the dead time of the digitizer. This is necessary before analysis to get the best possible resolution. Figure 5(a) below shows a raw output pulse from one of the CsI detectors. The raw pulse amplitude is approximately 600 mV and the pulse width is around 80 ns. The output pulse from all the CsI detectors had a considerably low amplitude and hence required amplification before being analyzed via the SIS3316 digitizer. Thus as seen in figure 6(a), the signal from CsI detector is passed through a timing and filter amplifier as the raw output signal of the detector did not fit any of the input bands of the SIS3316 digitizer. This also adds the 'gain' parameter to be optimised for each CsI detector which will be discussed further in the next section. The use of timing and filter amplifier is warranted as the signal not only needs amplification but also to set the shaping constant. The shaping constant(integrator) will be discussed in section 2.3.3. A seen in figure 5(b), the pulse width and amplitude from a single PMT of NaI(Tl) detector are approximately 500 ns and 600 mV respectively. This shows that the combined output of all PMTs of NaI(Tl) detector is sufficiently large enough to be analysed with the digitizer alone.

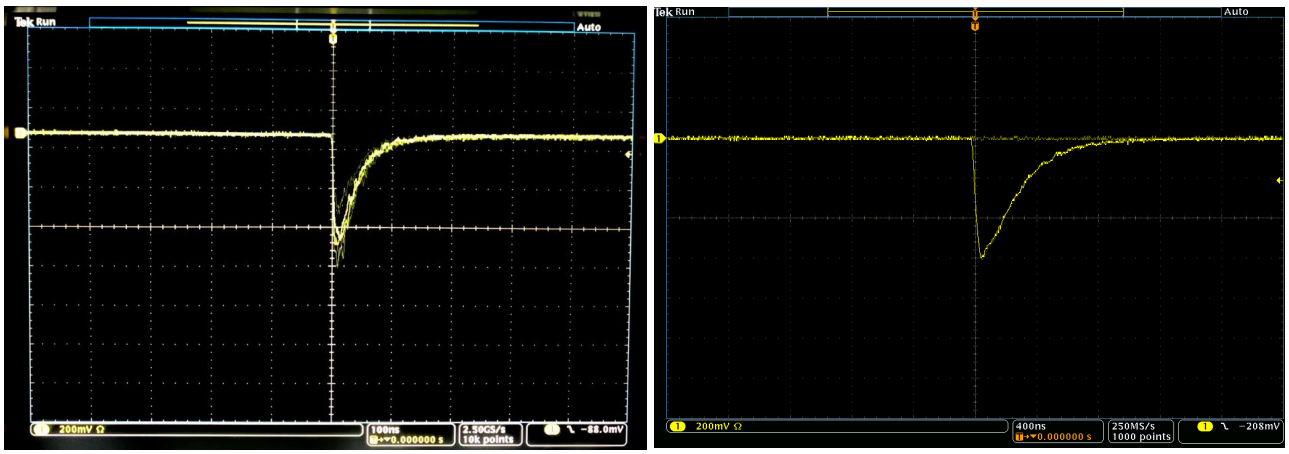

(a) CsI detector raw output pulse.

(b) NaI(Tl) detector single PMT raw output pulse.

Figure 5: Oscilloscope readouts for CsI and NaI(Tl) detector raw output.

Figure 6 below shows the schematics of CsI and NaI(Tl) detector setups. The CsI detector has a single crystal optically connected to a single PMT whereas the NaI(Tl) detector has a single crystal optically connected to four independent PMTs. Therefore, the outputs of all the four PMTs are combined into

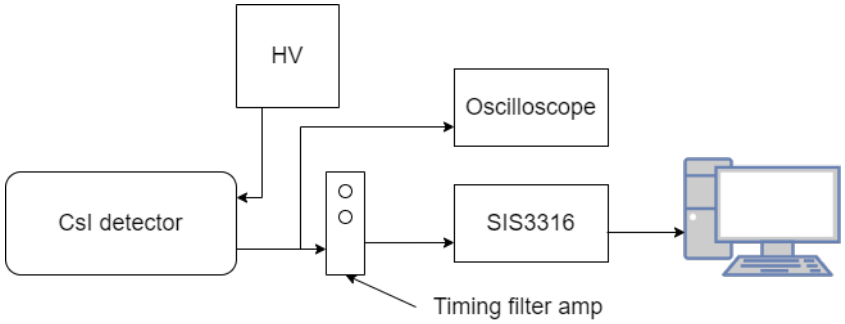

(a) Setup for CsI detector.

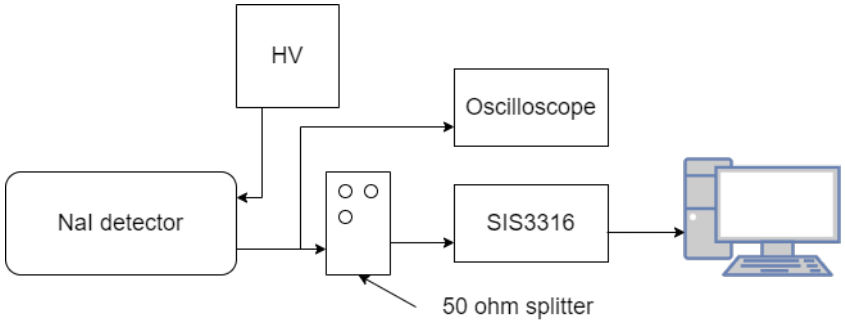

(b) Setup for NaI(Tl) detector.

Figure 6: Schematic diagragram for CsI and NaI(Tl) detector setups.

one single output signal. This was achieved by using combination of in-house built 50 Ω terminated signal splitters which act as passive combiners (figure 7). Two splitters combine the output of two PMTs into one and a third splitter combines the output of the the two splitters into one. This was done in a way as to not exceed the voltage capacity of the digitizer.

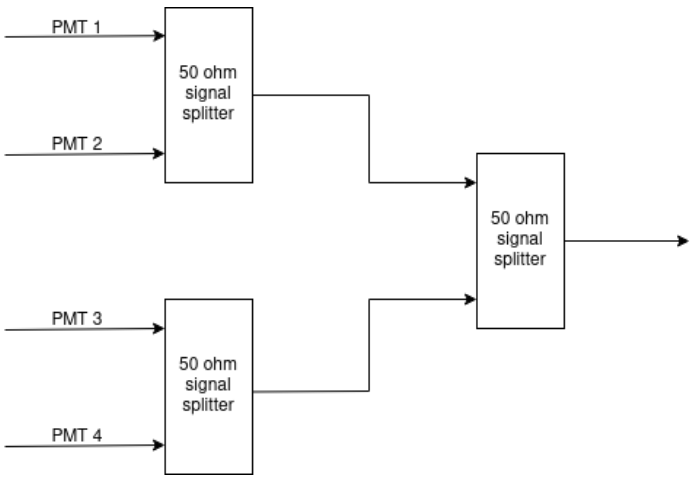

(a) Schematics for combining NaI(Tl) PMT signals.

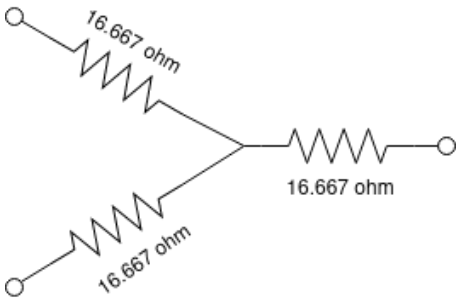

(b) Circuit diagram of 50 Ω terminated signal splitter.

Figure 7: Use of signal splitters as passive combiners for NaI(Tl) detector.

2.3 Parameter optimization

After having finalized the setup of our experiments, it is time to dive into optimizing the detectors. Each detector is unique when it comes to optimizing its experimental parameters despite having similar physical specifications. With the current experimental setup there are six parameters that need to be optimized before starting with data acquisition using these detectors. The parameters to be optimized in this research can be categorized into detector specific parameters and digitizer specific parameters (further referred to as systemic parameters). The detector specific parameters include the high voltage, integrator and gain (amplification factor) whereas the digitizer specific parameters include trigger threshold (TT) and accumulator widths. However, the signal amplitude of the NaI(Tl) detector is a combination of signals from four PMTs. Hence it is imperative to exclude the gain parameter i.e. the amplification of signal while using the NaI(Tl) detector.

Before proceeding it is necessary to acknowledge some of the environmental factors affecting the experiments. The laboratory in which the research was performed was below the ground level with close proximity to soil. This increases the background radiation. The detectors are old and salvaged from high energy experiments which make them prone to aging factors. The ageing factors include PMT deterioration, light leaks, etc.

2.3.1 High voltage

The potential difference between the dynodes of the PMT is determined by the applied high voltage. This high voltage dictates the amplitude of the output pulse. The most common modern day calibration method is the plateau measurement. The plateau measurement is performed using the detector to be tested, a suitable radioactive source and a rate meter. For a certain time period the counts of the source are recorded for a set high voltage using the detector. The process is repeated with increments in the applied high voltage to the detector. The plot of counts versus voltage reveals a plateau region where the number of counts is fairly insensitive to the change in the applied high voltage. The optimal operational high voltage is typically taken as the midpoint of the plateau section of the curve.

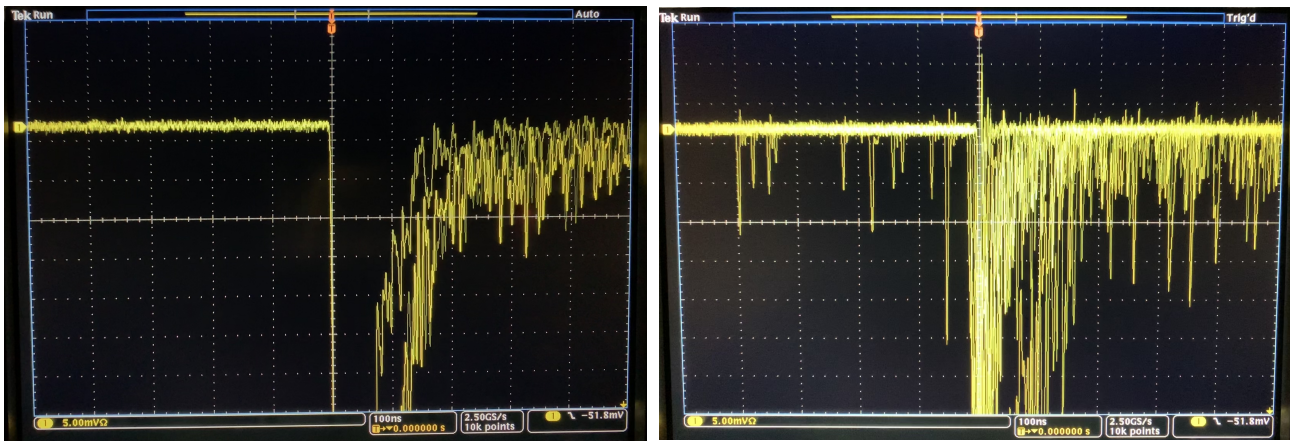

(a) No noise prior to leading edge.

(b) Noise induced prior to leading edge.

Figure 8: Snapshots of high voltage optimization using an oscilloscope.

However, because of the environmental factors, the high voltage for each detectors was measured by

a more practical approach instead of the plateau method. To determine the operational high voltages, we used an oscilloscope. For CsI detectors the high voltage was changed from -900V in 100V increments. The voltage beyond which we observed induced noise prior to the leading edge of the pulse was determined to be the optimal high voltage for the detector (figure 8). For the NaI(Tl) detectors we used the SIS3316 digitizer alone for the plateau measurement method. This was done due to the excellent output pulse characteristics combined with the sensitivity of the NaI(Tl) detector towards high voltages.

Detector	CsI no.0	CsI no.1	CsI no.2	CsI no.3
High voltage	-1300V	-1800V	-1700V	-1500V

Table 1: Optimized high voltages for CsI detectors.

NaI(Tl) PMT no.	0	1	2	3
High voltage	700V	675V	700V	665V

Table 2: Optimized high voltages for NaI(Tl) detectors.

2.3.2 Gain

This parameter denotes the amplification required to the output signal of the detector before it is analysed via digitizer. This is done to improve the resolution of the signal [6]. In this research, the main objective of amplifying the CsI detector signal is to improve the signal to noise ratio. As discussed in section 2.2, the raw output of the CsI detector is unsuitable to be processed by the digitizer. The internal electronic noise of the digitizer and the induced noise due to the other electronics is significant when compared to the raw output of the CsI detector. Amplifying the raw signal from the detector increases the signal amplitude while keeping the internal digitizer and other system induced noise insignificant for further processing thus improving the signal quality for further analysis. This research uses a timing and filter amplifier as it is also useful for manipulating the integrator (shaping constant) parameter. As the output amplitude of NaI(Tl) detector was already high enough to be analysed directly via the SIS3316 digitizer, it does not need this parameter optimized.

Figure 9 shows the comparison between sub-optimal and optimal values of gain for the detector CsI no.2. As seen in figure 9(b), the 511 keV peak of the ^{22}Na source is higher than the background peak. This value of $\times 12$ was later determined to be the best value of gain for CsI no.2 detector. However, in figure 9(a) the gain is set to $\times 20$. This high amount of amplification causes the signal peak to fall outside the maximum amplitude range of the SIS3316 digitizer.

Detector	CsI no.0	CsI no.1	CsI no.2	CsI no.3
Gain	12x	20x	12x	12x

Table 3: Optimized gain (amplification) for CsI detectors.

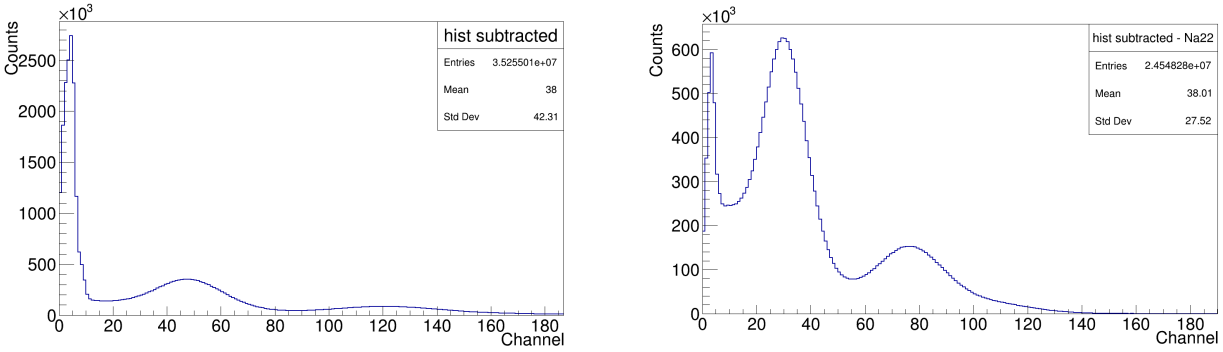

(a) Gain = $\times 20$ (b) Gain = $\times 12$

Figure 9: Comparison between suboptimal and optimal values of gain for CsI no.2 detector for ^{22}Na source.

2.3.3 Integrator (time constant)

For analyzing the detector output signal, it is necessary to improve the quality of the signal before passing it to the digitizer. The integrator is analogous to a low pass filter where the cutoff frequency is determined by the time constant. Visually, the integrator increases the pulse width. This is done to remove the high frequency noise from the signal. The higher the time constant, the lower is the cutoff frequency. However, increasing the time constant reduces the pulse amplitude while increasing the pulse width. Note that the overall integral of the area under the peak remains constant. Along with its function similar to a high pass filter, integrator is also used to adjust the pulse width of the raw output of the detector as to not fall within the deadtime of digitizer.

Accounting for the low pulse height and width of CsI detectors, two 10 minute measurements (with radioactive source and background) were performed with each CsI detector for a single value of time constant on the integrator. The subtraction of the background from source measurements, led to the determination of the optimal time constant for the CsI detectors. All the CsI detectors demonstrated the same optimised value of 50 ns. The integrator was a part of the timing and filter amplifier module. As the pulse width and height from NaI(Tl) detector were sufficiently large, it was also omitted from passing through an integrator.

2.3.4 Accumulator widths

The accumulator widths (gate widths) are parameters to be optimized in the SIS3316 user interface. These widths are representative of signal integration for the signal peaks. This tells the analysis code to integrate the area under the x-axis limits of the raw data window set by the user. The sampling rate of the digitizer is 250 MHz and the waveform length is set to 3000 samples. As the measurement performed is sample based, the conversion factor to time base is the inverse of sampling rate which is 4 ns.

The acquired data is still raw data and needs further refinement before analysis. Hence, after conversion to ROOT file format, an energy filter macro is used to generate the typical ‘counts vs energy’ histogram. This macro uses the accumulator widths to determine the area under the curve for peaks in the signal. Let the accumulator widths be W_1 and W_2. Now The operation of the energy filter can be expressed as as E_2/W_2 - E_1/W_1 where E_1 and E_2 are the summation of energy values covered by

the respective widths. The area under the energy peak thus can be perceived as the energy deposited in the bins within the range W_1 and W_2 normalised to the number of bins in the same range. Thus the energy integral (E_{int}) can be written as :

$$E_{\text{int}} = \frac{E_2}{W_2} - \frac{E_1}{W_1} \tag{1}$$

As seen in figure 9, the accumulator widths are set for baseline (W_1) (Length of accumulator 1) and the signal (W_2) (Length of accumulator 2). The selection for the peak width is that W_2 starts and ends at 5% of the maximum signal value. As for W_1 it starts from 0 and ends prior to start of W_2. Note that these widths can be considered as systemic parameters (digitizer based) rather than detector specific.

2.3.5 Trigger threshold

This parameter is also a systemic parameter (digitizer based) which is set in the SIS3316 GUI. This parameter only permits the recording and processing of the waveform signal above a certain value and is used to set a threshold for noise. This value is determined by viewing the signal in the MAW (Moving Average Window) filter window in the SIS3316 GUI (figure 10). This value is the lowest possible value at which the signal peak is distinctly visible in the MAW window. Any value lower than this value results in a noisy waveform with an indistinguishable signal peak. Also another criteria in deciding the value of threshold is that the two background subtraction or the background subtracted source spectrum should not have any negative values. This criteria is important as lower the threshold goes the count rate goes up and this can interfere with the deadtime of the digitizer.

Detector	CsI no.0	CsI no.1	CsI no.2	CsI no.3	NaI(Tl)
Accumulator width(W1)	0-400	0-400	0-400	0-400	0-365
Accumulator width(W2)	405-600	445-580	445-580	445-550	370-500
Trigger threshold	15	10	20	15	10

Table 4: Optimized digitizer based parameters for the tested detectors.

Figure 11 below shows the significance of trigger threshold values. The spectra are background subtracted. In figure 11(a) the trigger value is set higher (20) than the optimal determined value (15). This results in the suppression of counts for the measurement done with ^{22}Na source. The total registered entries by the detector with higher trigger values is $\approx$1.3 million whereas for the optimal value the total recorded entries are $\approx$23 million. The background energy distribution is constant in both measurements (with radioactive source and without). However, the addition of a radioactive source increases the count rate and signal amplitude while the dead time is constant. This may result in count overflow depending on the source. Along with high trigger values this suppresses the recording of background resulting in negative counts for background subtracted spectra.

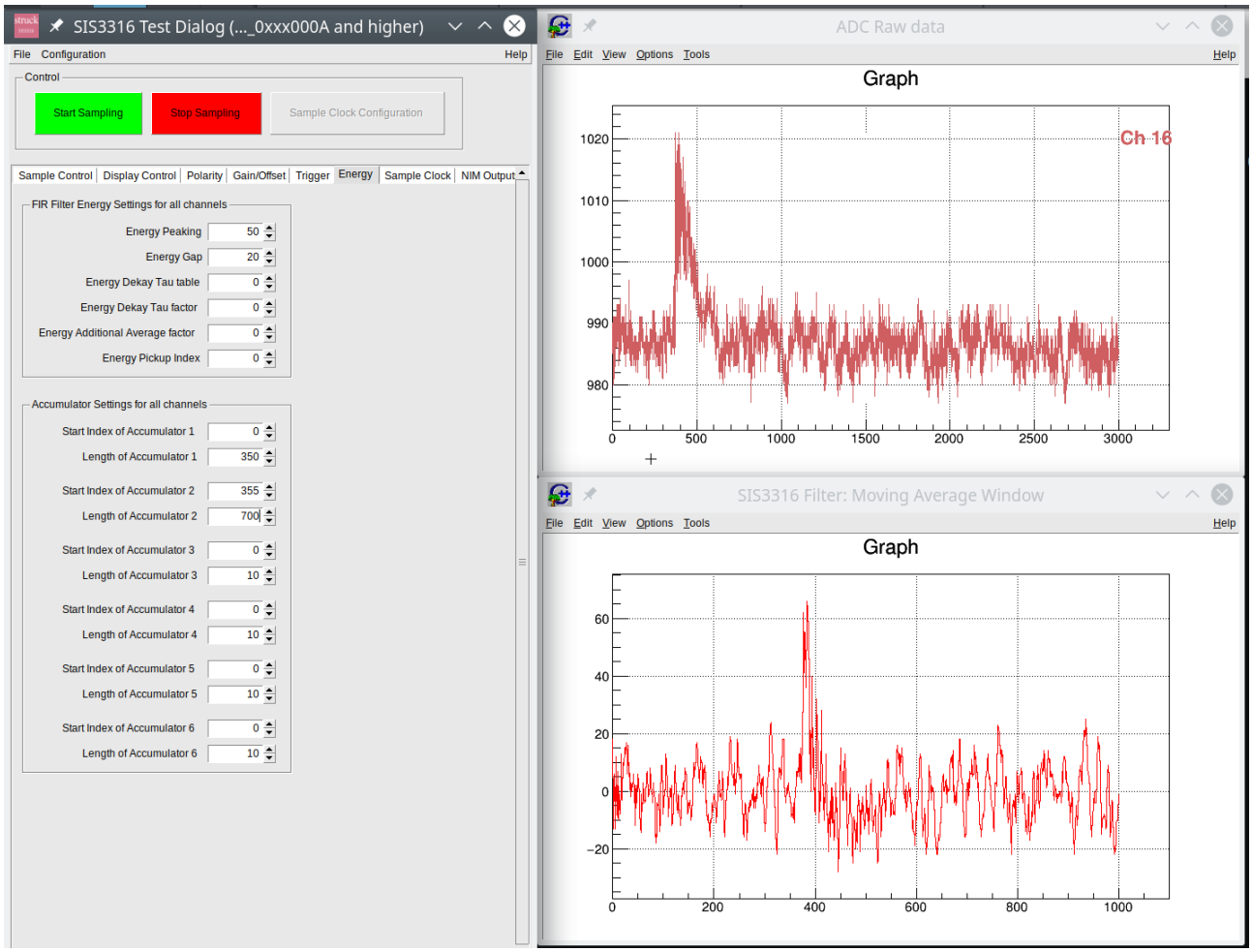

Figure 10: Energy settings tab (*left*) with ADC raw data (*top right*) and Moving Average Window filter (*bottom right*) in SIS3316 GUI.

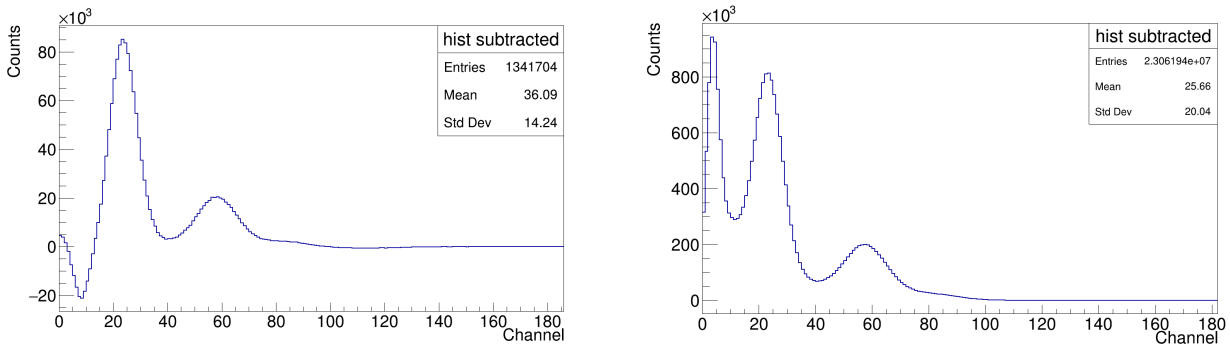

(a) Trigger threshold = 20 (arb. units).

(b) Trigger threshold = 15 (arb. units).

Figure 11: Comparison between suboptimal and optimal values of trigger threshold for CsI no.3 detector with ^{22}Na source

3 Methods and measurements

3.1 Data acquisition

With the optimized parameters for individual detectors and the setup described in section 2.2, the data acquisition was performed. For every detector, four measurements of 20 minutes were conducted. This also helps in reducing complexities during fitting procedure as the photo-peak energy distribution can be taken as a Gaussian distribution. For this research, two background radiation measurements along with one measurement with each radioactive source (^{22}Na and ^{60}Co) was done. For the measurements with a radioactive source, the source was kept at a distance of 5cm from the crystal end-cap of the detector.

Even though the SIS3316 is a 16 channel digitizer, the measurements were performed with one detector at a time. For every detector, a configuration profile unique to the detector was saved through the digitizer to verify the replicability of the experiment. This profile consists of the optimized parameters and digitizer settings unique to each detector. The documentation of this profile serves as the initializing protocols for every detector in case of future use in other experiments.

3.2 Data analysis

The data obtained from the digitizer is in generic data format (*.dat*) . The first order of business is to convert the data into proper format for analysis. In this research, the acquired data was first converted to ROOT [7] supported format (.root). For preliminary analysis of the data, the background measurement is subtracted from the measurement with the source. This gives a relatively clean spectrum for the respective radioactive sources as seen in figure 13. The next step in data analysis is to determine the energy resolution of the detectors.

The peaks obtained in the background subtracted spectra were fitted with a Gaussian fit. This was achieved using the ROOT software (*TBrowser*). The fitting procedure returns the sigma parameters along with the mean and other data for each energy peak of interest. Along with the calculations for energy resolution, the sigma parameters will later be useful in developing the simulations. The relative energy resolution (ΔE) can be calculated using the following relation [8]:

$$\Delta\mathrm{E} = \frac{\mathrm{FWHM}}{mean} = \frac{2.355 \times \sigma}{mean} \times 100\% \tag{2}$$

Note that the errors obtained during acquisition of *sigma* and *mean* parameters from the calibrated spectra are of the order of 10^{-3} to 10^{-4}. The resulting error propagation for energy resolution comes out to the order of 10^{-4} and thus can be neglected in further discussion. The error propagation (ρ) was calculated using the following relation:

$$\rho = \frac{\delta(\Delta\mathrm{E})}{\Delta\mathrm{E}} = \sqrt{\left(\frac{\delta\sigma}{\sigma}\right)^2 + \left(\frac{\delta(mean)}{mean}\right)^2} \tag{3}$$

In this research the known energy peaks obtained from ^{60}Co (1173.2 keV and 1332.5 keV)and ^{22}Na (511 keV and 1275 keV) were used for calibration. After obtaining the baseline (background) subtracted spectra and the sigma parameters, the known values of energies for corresponding peaks are divided by the *mean* (channel) values obtained during the Gaussian fitting of the peaks. The energy per channel (E_{ch}) values for NaI(Tl) and CsI detectors were 16.76 keV for NaI(Tl) and 16.98 keV for *CsI no.2*. Using these values the obtained data was calibrated for every detector.

$$\mathrm{E}_{ch} = \frac{\mathrm{E}_{peak}}{mean} \tag{4}$$

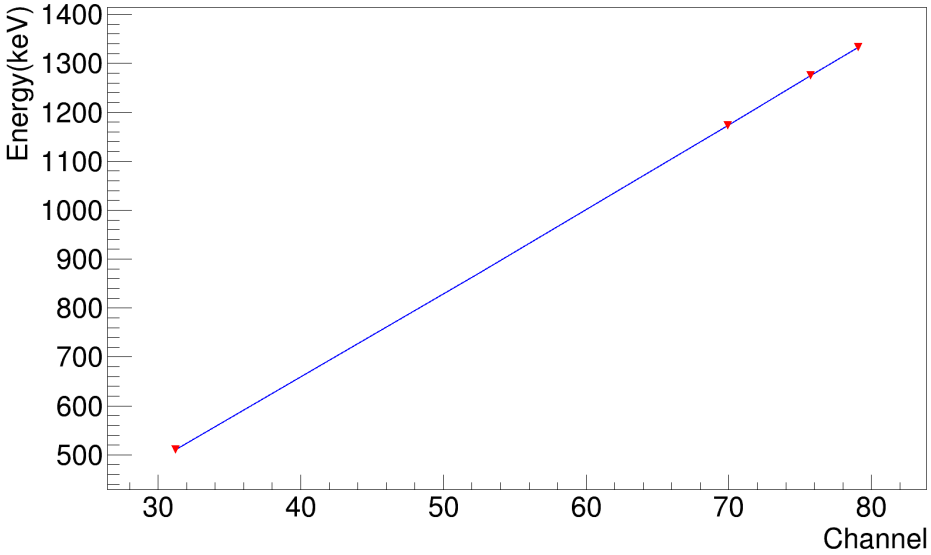

Figure 12: Energy - channel calibration curve for NaI(Tl) detector using ^{60}Co and ^{22}Na energy peaks.

The figure 13 below chronologically depicts the various steps of data processing from data acquisition to obtaining calibrated spectra for NaI(Tl) detector using ^{60}Co as source.

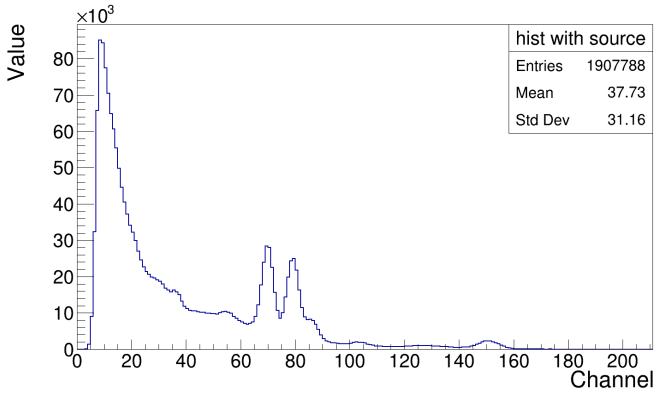

(a) ^{60}Co measurement with background.

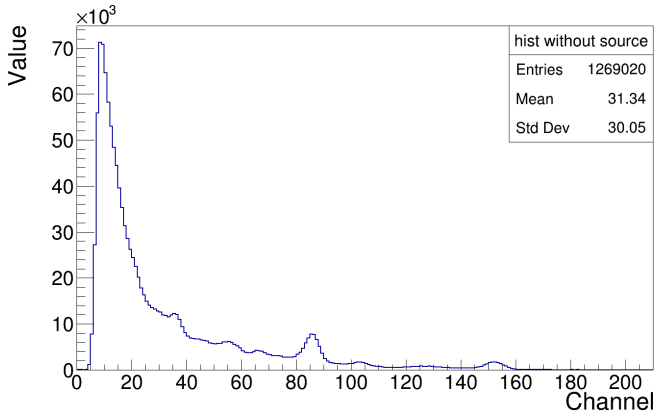

(b) Background measurement.

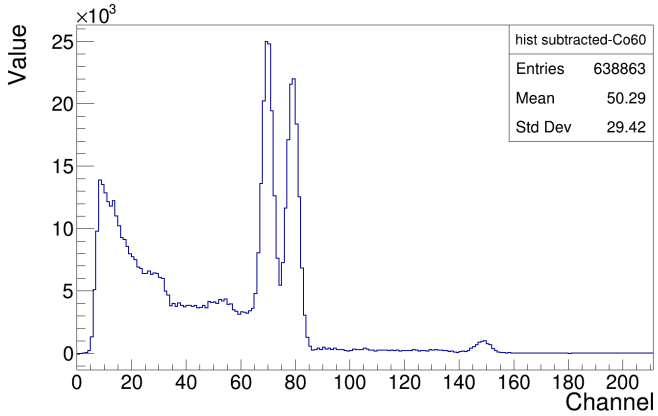

(c) Uncalibrated ^{60}Co spectra with subtracted background.

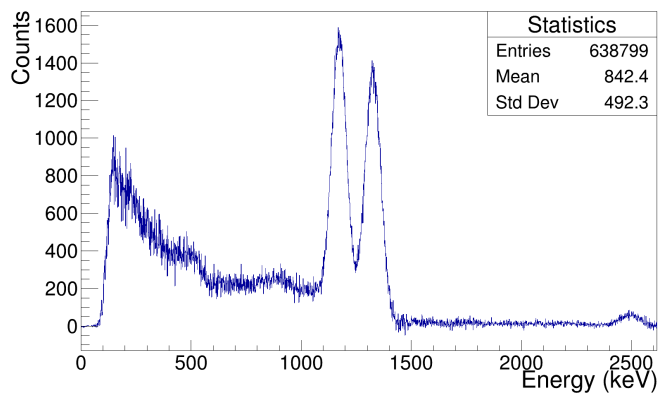

(d) Energy calibrated ^{60}Co spectra.

Figure 13: Data acquisition and processing steps in measured ^{60}Co spectrum using NaI(Tl) detector.

4 Simulation environment

The objective of this research is to determine the viability of CsI and NaI(Tl) detectors to be used in a GAINS-like setup. It is thus necessary to have a comparison between data sets acquired from both the GAINS and the CsI or NaI(Tl) based GAINS like setups. To do this without constructing the actual setup with CsI or NaI(Tl) detectors, this research uses GEANT4 [4] based simulations of GAINS and GAINS-like setup using CsI and NaI(Tl) detectors.

4.1 GEANT4

GEANT stands for **GE**ometry **AN**d **T**racking and the number represents the version. It is an object oriented toolkit for Monte Carlo simulations designed for simulating passage of particles through matter. It is written in C++. Along with geometry and tracking, GEANT4 (further referred to as G4 for convenience) includes all aspects of simulation process like fundamental particles, event and track generation with storage, materials used, physics governing particle interactions, visualization of detectors and trajectories and lastly capture, analysis and refinement of simulation data. All this can be done over a wide energy range. In short, G4 can be used to study and visualize a wide range of experiments from a single phenomenon to full-scale detector simulations at $\overline{\text{P}}$ANDA , LHC etc [9].

4.2 Simulation development

To develop a simulation using G4, the first hurdle is to replicate the existing detectors' setup as precisely as possible. Even though the G4 libraries have all the materials and necessary physics of particle interactions, not all detectors made of same material have the exact same characteristics. In case of this research, the physical geometry of all the detectors is the same with the crystal material being the only changing factor to affect the simulation. But, as seen from the calculated energy resolutions (table 6), every CsI detector behaves differently.

The energy response function is a Gaussian for the detectors in this research. This standard deviation of this Gaussian depends on the incident energy. This relationship between the incident aenergy and the standard deviation of the Gaussian can be expressed in terms of a polynomial. To keep things simple this research uses a second degree polynomial of the nature :

$$\sigma(E) = a\mathrm{E}^2 + b\mathrm{E} + c \tag{5}$$

Where E denotes the energy of photo-peak, σ denotes the sigma parameter (standard deviation) corresponding to the photo-peak energy E and a, b, c are the parameters to be derived for simulations. The values of σ for corresponding E were found during the fitting procedure described in section 3. However, the CsI detectors were unable to resolve the adjacent ^{60}Co energy peaks. This led to having two equations with three unknowns. Hence, a linear fit function was used to derive fit parameters for CsI detectors as follows:

$$\sigma(E) = b\mathrm{E} + c \tag{6}$$

These function fits were used to derive parameters unique to individual detectors based on the experimental results obtained from each detector. These along with precise physical measurements and use of proper materials from the G4 library were used in development of the first simulation. The first simulations were performed in the exact way to the single detector experiments conducted in the laboratory; the only difference being that the laboratory experiments were timed measurements whereas the simulations were generated with predefined counts of radioactive decay of the source. However, for the NaI(Tl) detector, the use of equation 5 led to four equations with three unknowns. Solutions generated from solving three equations need not necessarily satisfy the fourth one. Hence, the necessary parameters were extracted from fitting the plot of σ vs energy for NaI(Tl) (figure 14). These extractions were performed by linear fit which gave the parameters to satisfy equation 6.

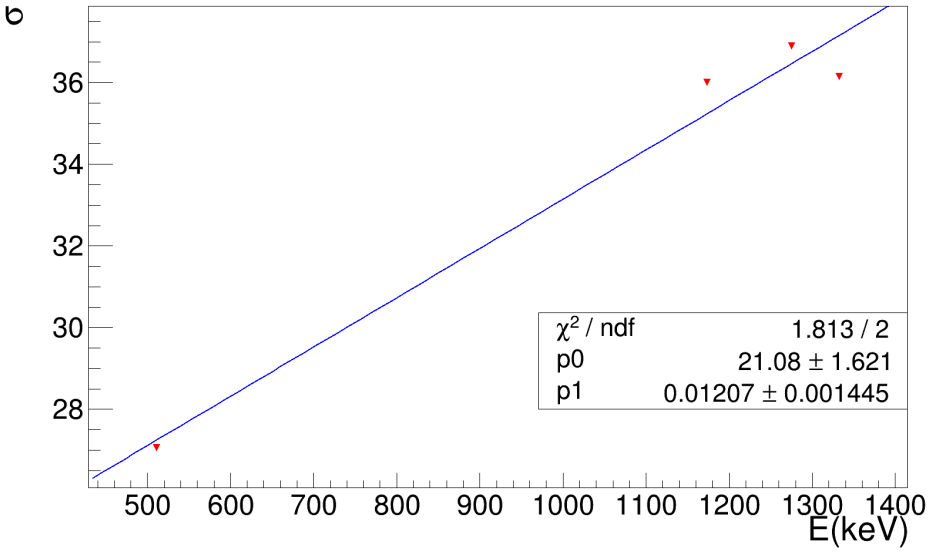

Figure 14: σ vs energy for NaI(Tl) detectors.

Data acquisition and analysis was conducted from the simulations. The analysis was done by comparing the simulation based data to the experimental data figure (15). This was done in order to verify and/or improve on the derived fit parameters as to replicate the real life detectors as precisely as possible. As seen in the extract from the simulation figure 16(a), colored lines signify various particle trajectories(γ (green), electrons (red) etc.) and yellow points signify particle interactions.

4.3 Data acquisition and analysis

After verification of fit parameters, the next step is to simulate the GAINS setup with twelve HPGe detectors. The parameters for HPGe detectors were obtained from data provided for this research. The simulated GAINS spectrometer can be seen in figure 16(b). Along with HPGe similar geometry setups made using CsI and NaI(Tl) detectors were simulated figure 16(c) from the derived parameters for the respective detectors. For data acquisition with GAINS like setups , it was decided to have the two twelve detector setups (HPGe-NaI(Tl) or HPGe-CsI) be facing each other. The simulation was run using isotropic point sources (^{60}Co, ^{22}Na) placed at the centre of the two rear hemispherical detector setups figure 16(c). Special attention was given to keeping the source equidistant from all the

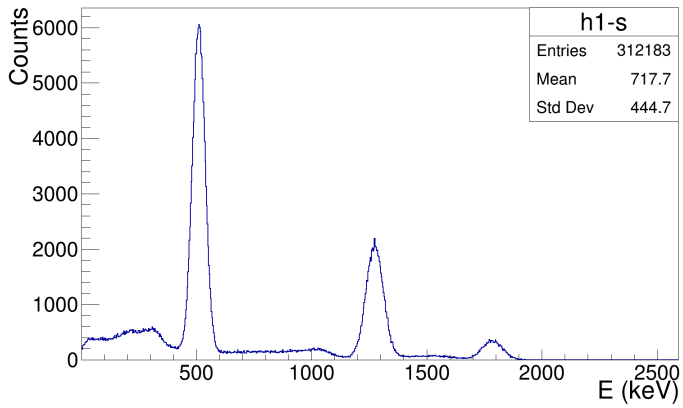

(a) Simulated spectrum.

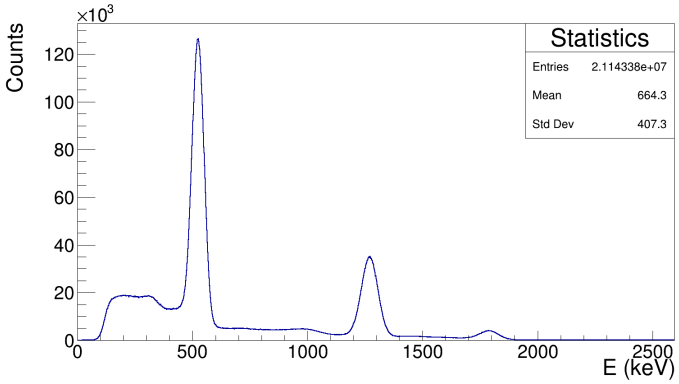

(b) Experimental spectrum.

Figure 15: Comparison between simulated and experimental spectrum of ^{22}Na from single NaI(Tl) detector.

detectors in one set irrespective of the distance and or orientation between the two detector setups. The data acquisition for both twenty four detector setup simulation was performed with 5×10^5 events. The simulation run generates a root file. The root file is processed with the proper smoothing function (equation 6) implementing the derived fit parameters for the respective detector. Along with generating a waveform spectrum, a text file was generated by extracting the number of counts detected per channel. This was done in order to calculate the efficiency of the detector setup which will be discussed in the next section.

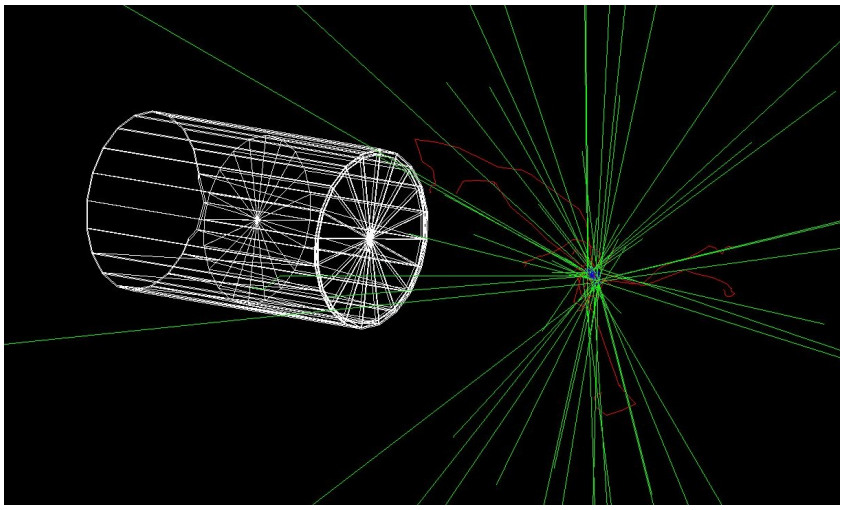

(a) Single detector simulation using GEANT4.

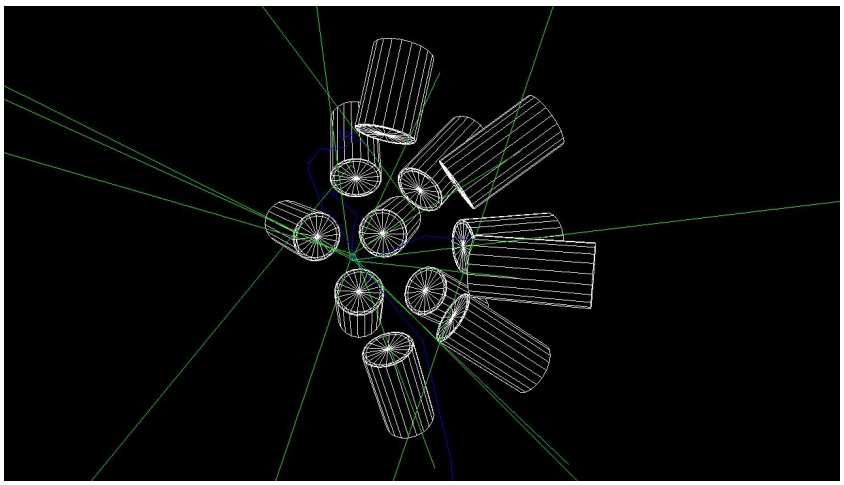

(b) 12 HPGe detector based GAINS spectrometer simulation.

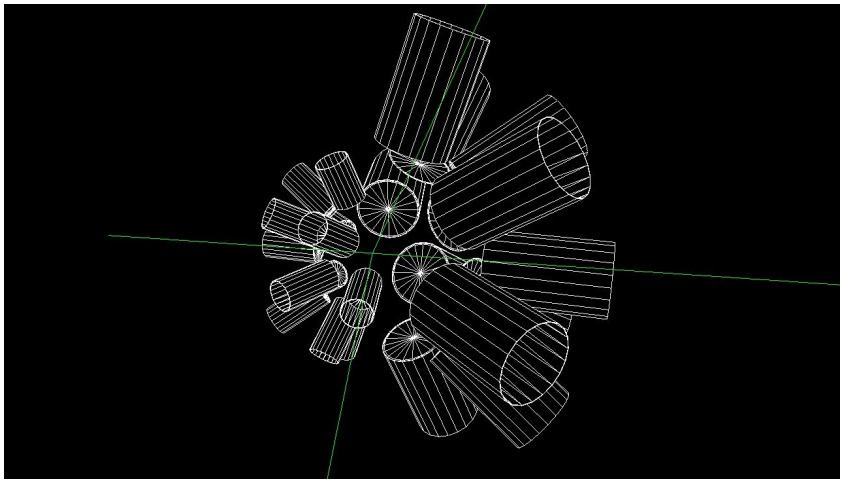

(c) GAINS spectrometer (*left*) and NaI(Tl) based GAINS like detector setup (*right*) with a radioactive source in the middle.

Figure 16: Snapshots of detector setups' development in G4 simulation environment.

5 Results and discussion

This section consolidates all the results of the work done in this research. The goal of this research is to access the viability of the CsI and NaI(Tl) detectors to be used in GAINS-like configuration at GELINA. This research is focused on energy dependent characteristics of the said detectors.

5.1 Experimental results

In this study one NaI(Tl) and four CsI detectors were characterized and optimized. Each detector was tested with two radioactive sources; ^{22}Na and ^{60}Co. With this work, it was possible to develop a protocol for initializing and calibrating the said detectors for future use in experimentation and education.

5.1.1 CsI detectors:

The optimized parameters for all the CsI detectors can be seen in table 5 below. Note that the trigger threshold and accumulator widths are digitizer (SIS3316) based and should be optimized anew when using with other ADCs or even if using another module of SIS3316. The remaining parameters are detector specific and can be used to initialize the detectors when used in other experiments. In this section, emphasis is given to results from individual detectors.

Detector	CsI no.0	CsI no.1	CsI no.2	CsI no.3
High voltage	-1300V	-1800V	-1700V	-1500V
Integrator	50 ns	50 ns	50 ns	50 ns
Gain	12	20	12	12
Trigger threshold	15	10	20	15
Accumulator width(1)	0-400	0-400	0-400	0-400
Accumulator width(2)	405-600	445-580	445-580	445-550

Table 5: Optimized parameters for CsI detectors.

In case of the detector *CsI no.0*, as seen in figure 17 below, the detector was unable to resolve energy peaks for ^{22}Na. This detector was also tested with ^{60}Co. However, it was unable to resolve any energy peaks. This might be due to various factors like crystal ageing, light leak, bad PMT etc. This renders the detector of no use in this study as it is impossible to measure the energy resolution or derive fit parameters for the simulations. Hence, this detector is discarded from further discussions. The low energy resolution of the CsI detectors is responsible for the broad energy peaks. In figures 17 - 19 below, the calibrated spectra for ^{60}Co and ^{22}Na can be seen as observed by individual CsI detectors. As seen in the figure 20(a), the ^{60}Co spectra has negative counts when it comes to the background noise region. This issue was investigated during the experimentation stage. Multiple background

measurements and source measurements were made using ^{60}Co and ^{22}Na. However, the ^{22}Na spectra came out similar to figure 20(b).

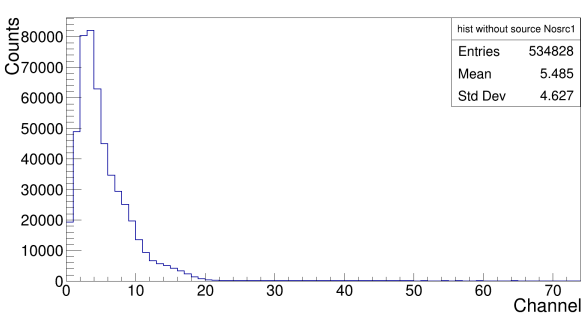

(a) Background measurement.

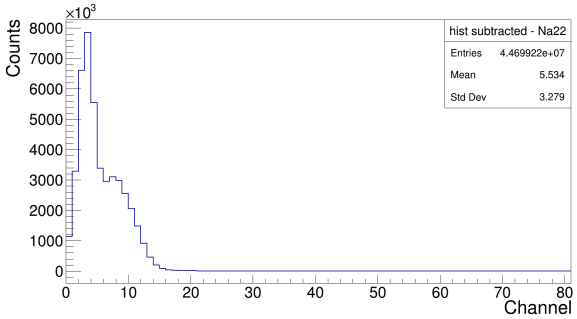

(b) Measurement with ^{22}Na as source.

Figure 17: Data obtained from detector CsI no.0 .

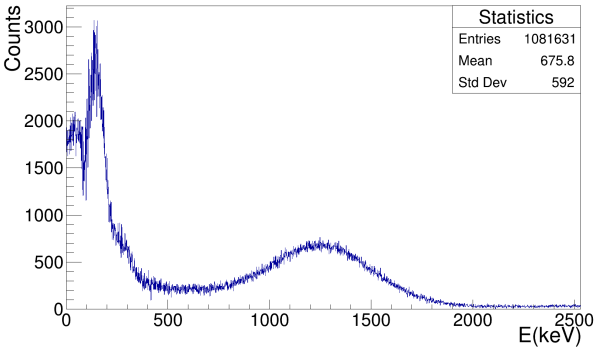

(a) ^{60}Co spectrum.

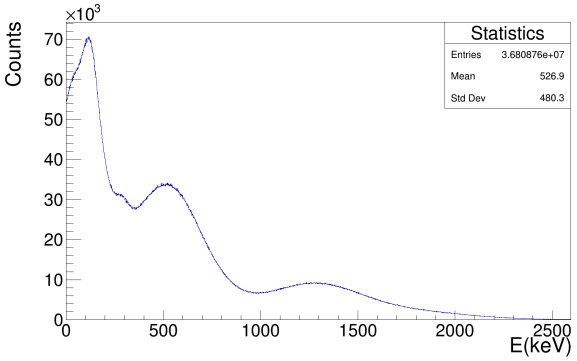

(b) ^{22}Na spectrum.

Figure 18: Calibrated data from detector CsI no.1 .

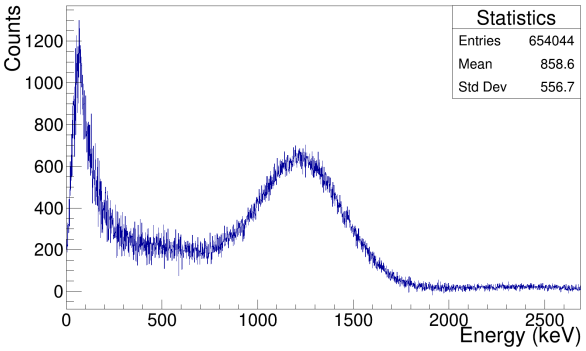

(a) ^{60}Co spectrum.

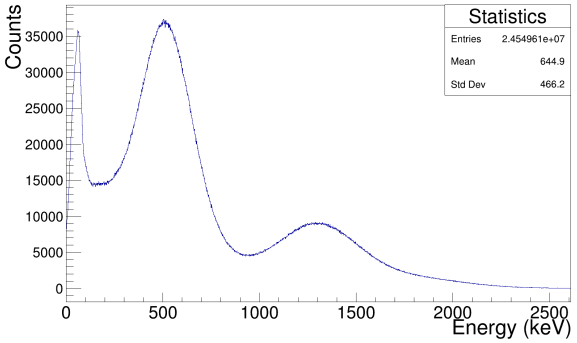

(b) ^{22}Na spectrum.

Figure 19: Calibrated data from detector CsI no.2 .

But with ^{60}Co as source, all the subtracted and calibrated spectra showed the same trend as in figure 20(a). This can be due to many factors like crystal deterioration, bad PMT, weak source etc. To get to

the root cause, many approaches were tried including rechecking the optimized parameters. But after connecting the detector to a rate meter, it was observed that the detector had an overflow of counts with the ^{60}Co source. This meant that the dead time of the detector was high and the consecutive hits occurring within the dead time of the detector were not recorded. This explained the negative counts in the background subtracted spectra. For rectifying, the trigger threshold was increased from 15 to 20 (arbitrary units in SIS3316 GUI). The results from this modification can be seen in figure 21. The background subtracted spectrum shows a significantly reduced background signature compared to the old spectrum with lower threshold. Still, the ^{60}Co peaks were unresolved. The auxiliary data was not calibrated as:
(1) The visual cues from the spectrum represent the poor energy resolution of the detector (merged ^{60}Co peaks).
(2) The change in trigger threshold parameter values with change in source implies the unreliability of the detector to be used for complex gamma spectra with variable interaction rates for different energies.
Although the energy resolution for *CsI no.3* based on ^{22}Na spectra was best amongst the ensemble of CsI detectors by a sufficient margin, due to its unreliability, the detector *CsI no.3* was discarded in simulation development.

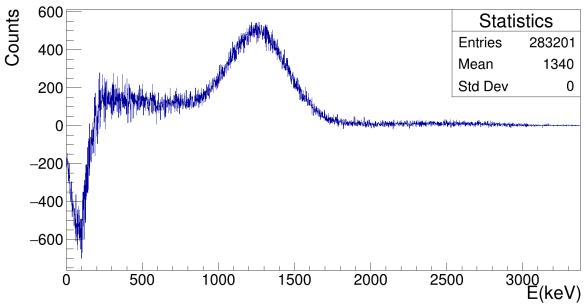

(a) ^{60}Co spectrum.

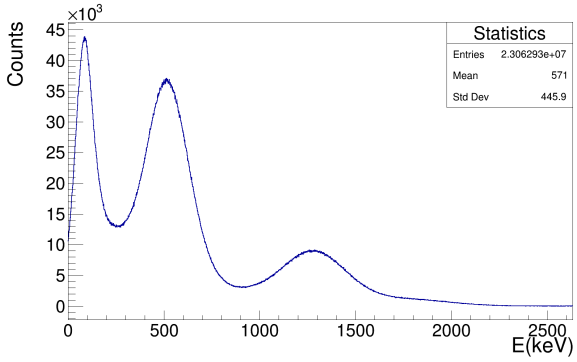

(b) ^{22}Na spectrum.

Figure 20: Calibrated data from detector CsI no.3 .

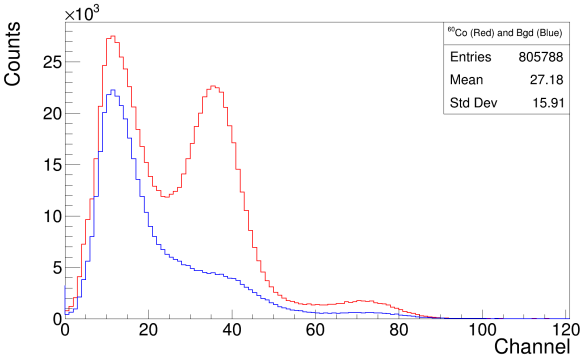

(a) ^{60}Co spectrum (red) with background (blue).

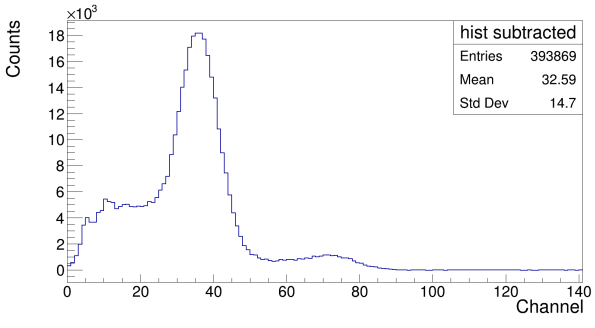

(b) Background subtracted ^{60}Co spectrum.

Figure 21: Auxiliary ^{60}Co data from detector CsI no.3 with modified threshold parameter .

5.1.2 NaI(Tl) detector

As discussed in section 2, the NaI(Tl) detector signal is comprised of combined signal of four PMTs. The optimization parameters for this detector include the detector based parameter of individual high voltages for each of the four PMTs (*table 2*) and the digitizer based parameters of accumulator widths and trigger threshold (*table 4*). The background subtracted and energy calibrated spectra for ^{60}Co and ^{22}Na as recorded by the NaI(Tl) detector can be observed in figure 22 below. The NaI(Tl) detector has shown superior energy resolution and operational condition compared to CsI detectors.

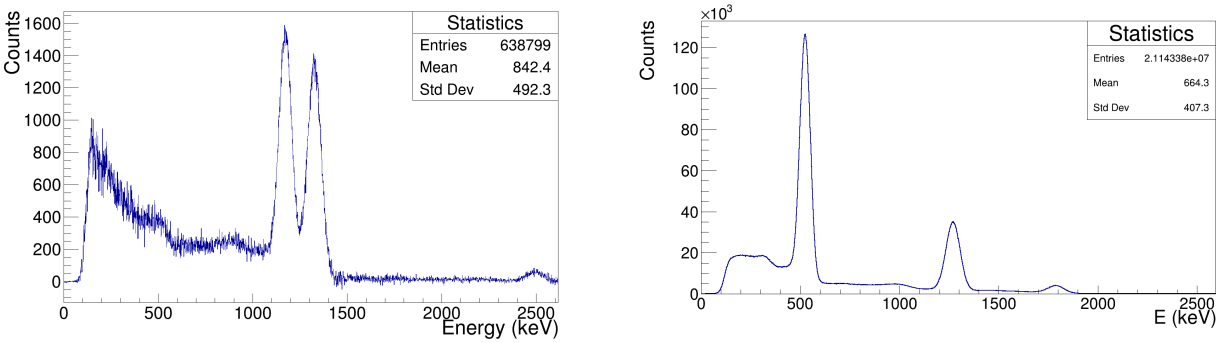

(a) ^{60}Co spectrum.

(b) ^{22}Na spectrum.

Figure 22: Calibrated data from NaI(Tl) detector.

5.2 Energy resolution

The procedure for calculation of energy resolution was described in section 3.2. The energy resolution of a detector is its ability to resolve two peaks of relatively close energies. High energy resolution (small FWHM) implies higher definition of individual energy peaks [6]. This translates into the fact that the lower the percentage values, the higher the energy resolution. It is more desirable to have high energy resolution for complex gamma spectrum. For example in a complex gamma spectrum like ^{239}Pu some information on close energy photo-peaks may be lost due to lower energy resolution (broader merged peaks).

The calculated energy resolution of all the detectors can be seen in table 6 below. Note that none of the CsI detectors were able to resolve the close proximity energy peaks of ^{60}Co with corresponding energies of 1173.2 keV and 1132.5 keV. In contrast NaI(Tl) detector was able to resolve all the energy peaks of ^{60}Co and ^{22}Na. Thus it is safe to say based on acquired data that CsI detectors (used in this study) are unsuitable to be used in GAINS-like setup. As none of the sources have a complex gamma spectrum, the decision on viability of using NaI(Tl) detectors in GAINS-like configuration will depend purely on the scope of planned experiments.

Energy resolution				
Energy (keV)	CsI no.1	CsI no.2	CsI no.3	NaI(Tl)
511	95.58%	70.41%	56.49%	12.16%
1275	55.72%	44.47%	35.19%	6.84%
1173.2	NA	NA	NA	7.23%
1332.5	NA	NA	NA	6.42%

Table 6: Calculated Energy resolution of all detectors.

5.3 Simulation results

A single detector simulation spectrum was seen in section 4.2 figure 15(a). The previous section concluded with simulation development of a twenty four detector setup [12× HPGe(GAINS) and 12 × NaI(Tl) or CsI(GAINS-like)]. The CsI based GAINS-like setup uses simulation parameters derived from detector *CsI no.2*.

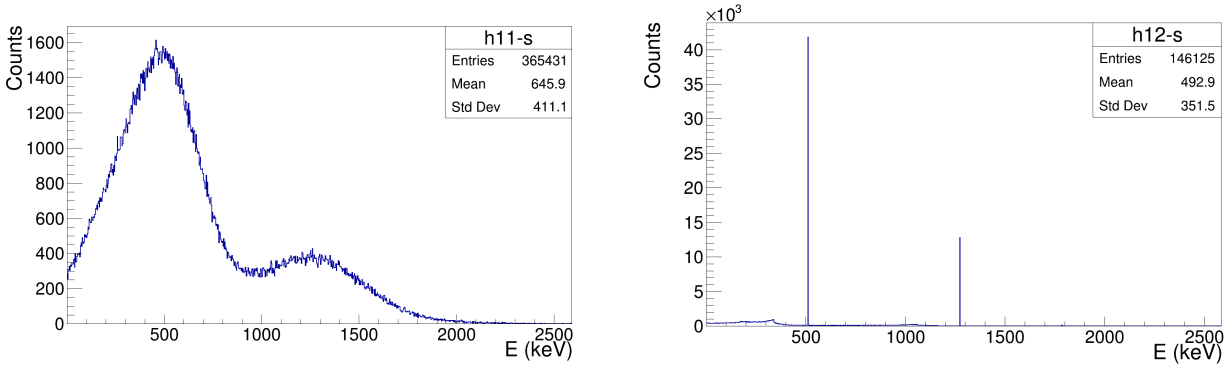

(a) Simulated Na22 spectrum from CsI no.2.

(b) Simulated Na22 spectrum from GAINS.

Figure 23: ^{22}Na simulated spectra comparison between CsI detectors and GAINS.

Note that, as seen in experimental results the CsI detectors were unable to resolve the ^{60}Co peaks and as the simulation reflects the experiments, it would be futile to show the simulation results for ^{60}Co. As only HPGe simulations will have resolved energy peaks. Also, the background is not modelled in the simulations. Figure 23 depicts the poor performance of CsI based GAINS-like detector setup in comparison to HPGe based GAINS. The broad peaks for 511 keV and 1275 keV seem to be merged around 1 MeV mark for the CsI detector based setup. This implies that CsI based GAINS would not be able to resolve complex gamma spectra. Hence based on resolution alone, it is fair to say that use of CsI detectors in GAINS-like setup is not suitable.

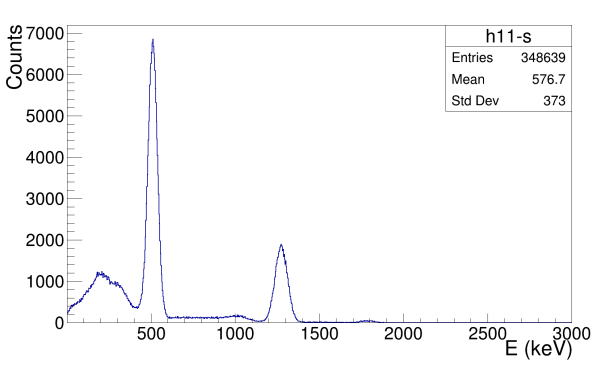

(a) ^{22}Na spectrum simulated with NaI(Tl).

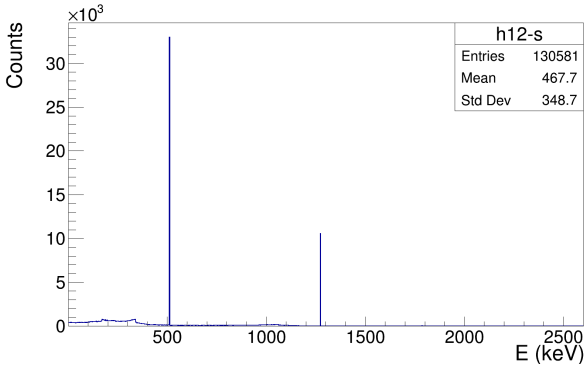

(b) ^{22}Na spectrum simulated with HPGe.

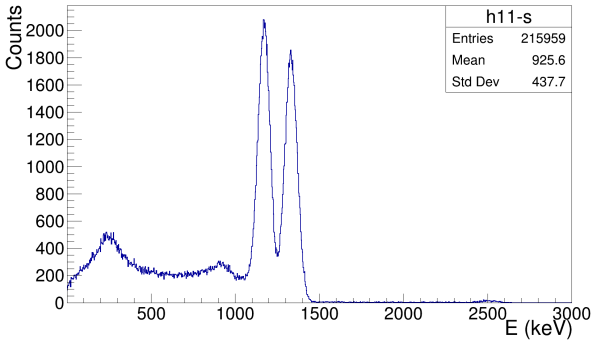

(c) ^{60}Co spectrum simulated with NaI(Tl).

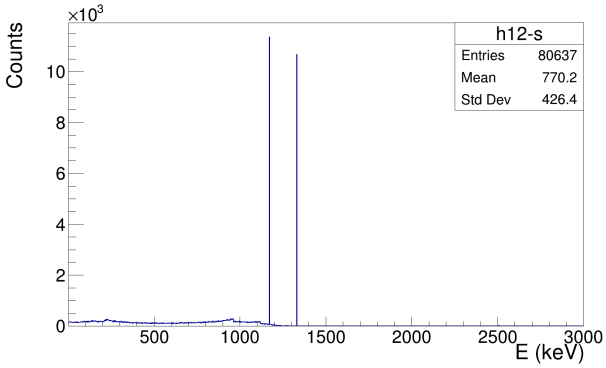

(d) ^{60}Co spectrum simulated with HPGe.

Figure 24: Simulated spectra comparison between NaI(Tl) GAINS-like setup and GAINS.

From the figure above figure 24, The NaI(Tl) based GAINS-like setup was able to resolve all the energy peaks of ^{60}Co and ^{22}Na. The NaI(Tl) detector resolution is between 88 keV - 90 keV for corresponding energy range of 1 MeV - 1.4 MeV. Although this is not as good as HPGe detectors, it is not possible to refute the use of NaI(Tl) detectors in GAINS like setup unless the scope of experiments is taken into account.

5.3.1 Detector setup efficiency

In the GAINS spectrometer, every detector is almost equidistant from the source with a possible variance of few millimeters. The efficiency calculations conducted in this study are based on the data acquired from mono energetic simulations of twelve detector setups modelled after a single detector of each type. Also, the rear-hemispherical configuration makes it harder to calculate the absolute efficiency of the entire setup. With the geometric efficiency being almost the same for all detectors in a particular setup, only intrinsic efficiency would have significant effect on the total efficiency of the setup. Hence, this study focuses only on the intrinsic efficiency of simulated GAINS and NaI(Tl) based GAINS-like setup.

The intrinsic efficiency of a detector is the ratio of the number of counts recorded (N_{rec}) by the detector to the number of particles impinging on the detector (N_{imp}) (*equation 7*). In this study, the intrinsic efficiency for NaI(Tl) based GAINS-like setup was calculated for energy range of 0.5 MeV to 4 MeV. This efficiency curve is compared to simulation based GAINS efficiency curve for the same

energy range. It can be seen in figure 25 that the NaI(Tl) based GAINS-like setup has better efficiency curve compared to current HPGe based GAINS.

$$\varepsilon_{\text{int}}(E) = \frac{N_{rec}}{N_{imp}} \times 100\% \tag{7}$$

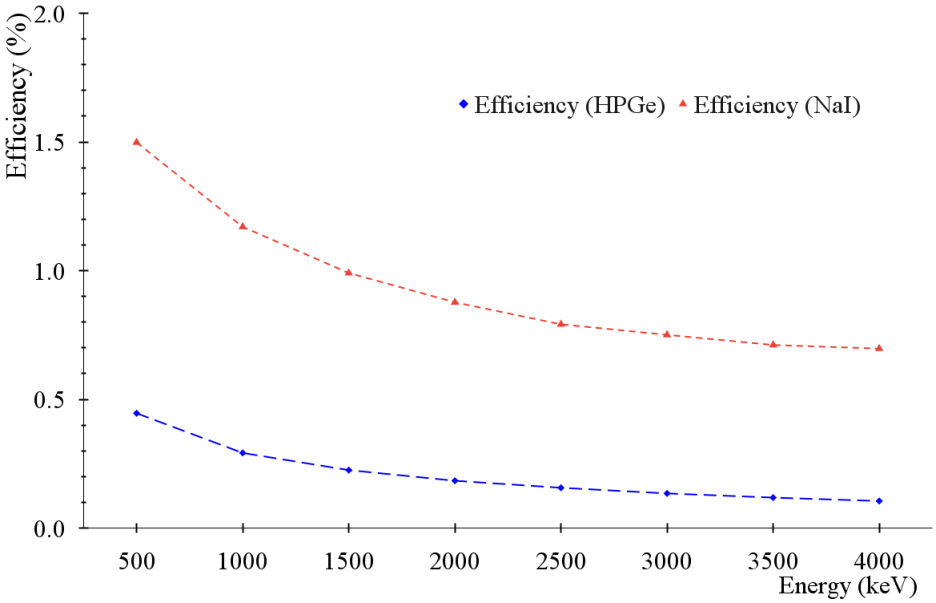

Figure 25: Efficiency comparison for GAINS and NaI(Tl) based GAINS-like setup.

One of the factors affecting the discrepancy in efficiency between the GAINS and NaI(Tl) based GAINS-like setup is the geometry of the detector setup. The diameter of the HPGE crystal in the GAINS detector setup is 8 cm whereas the diameter of the NaI(Tl) crystal used in the experiments for this thesis is 21 cm. The distance between the gamma source and the NaI(Tl) and that between the source and HPGe detectors in the 24 detector G4 simulations is 35 cm and 18 cm respectively. This leads to the fact that the solid angle subtended by any one of the NaI(Tl) detectors to the point source ($\Omega_{NaI(Tl)}$) is 0.28 sr and the solid angle subtended by any one of the HPGe detectors to the point source (Ω_{HPGe}) is 0.15 sr. The ratio of $\Omega_{NaI(Tl)}$ to Ω_{HPGe} is 1.86. At 500 keV the ratio of efficiency of NaI(Tl) based GAINS-like setup ($\varepsilon_{NaI(Tl)}$) to the efficiency of HPGe based GAINS setup (ε_{HPGe}) is 3.36 (figure 25). Thus, it can be stated that at 500 keV, the efficiency of NaI(Tl) based GAINS-like setup is better than that of HPGe based GAINS by a factor of 3.36 out of which the geometry (larger crystal size) of the NaI(Tl) detector contributes a factor of 1.86.

The further quantification of the gain in efficiency of NaI(Tl) based GAINS-like setup compared to HPGe based GAINS is done in figure 26 below. The efficiency of NaI(Tl) based setup and GAINS is first normalized to the solid angle and the ratio of $\varepsilon_{NaI(Tl)}$ to ε_{HPGe} gives the normalized efficiency gain for a direct comparison. The efficiency gain for all simulated energies shows a declining trend of efficiency gain towards higher energies. That being said, for the energy range between 500 keV and 4 MeV; which is the most crucial range for GAINS related experiments; the efficiency gain of NaI(Tl) based GAINS-like setup falls from 16% to 8%. This goes to show that NaI(Tl) based GAINS-like setup is viable for the said energy range depending on the nature of the experiment.

The efficiency gain normalized to the solid angle is calculated as per equation 8 below:

$$\varepsilon_{\text{gain}} = \frac{\varepsilon_{NaI(Tl)}}{\varepsilon_{HPGe} \times 1.86} \times 100\% \tag{8}$$

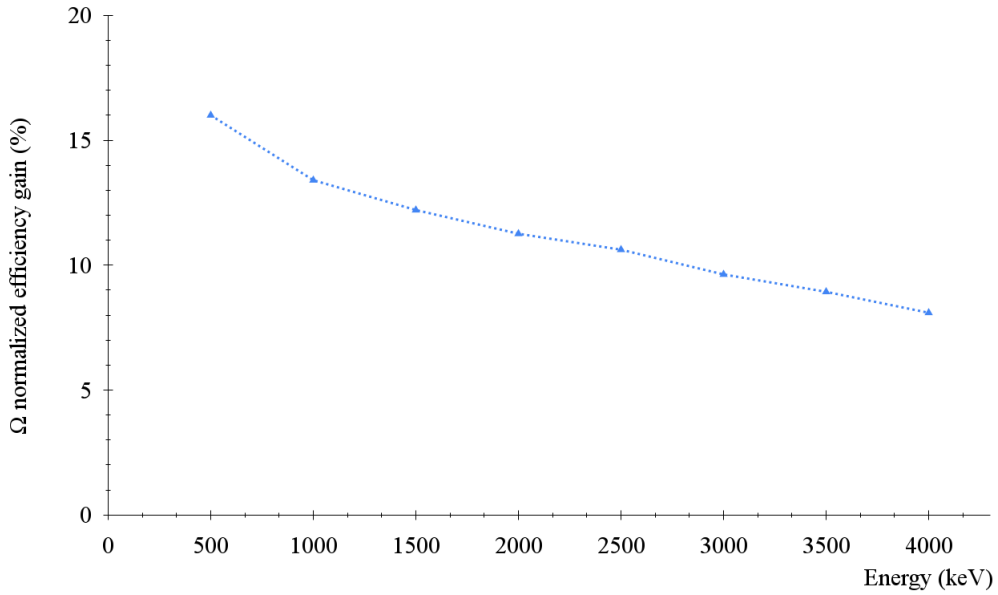

Figure 26: Solid angle (Ω) normalized efficiency gain for NaI(Tl) based GAINS like setup.

6 Conclusion

With increasing reluctance to be dependent on conventional fuels, many nations are turning towards nuclear energy. Although many countries field nuclear reactors due to their evident advantages, there are always concerns regarding nuclear waste, safety and economic feasibility. The GAINS spectrometer was developed in order to study peculiar subatomic transitions of interest for development of generation four molten salt reactors (MSRs). With curiosity being the driving force of scientific minds, one question always pops up, " is it possible to do it in a better way?".

GAINS spectrometer is built with twelve HPGe detectors. HPGe detectors have excellent energy resolution. However, they are troubled with problems like smaller crystal size, high cost and low operating temperatures which increases their operational costs. As seen in the twenty four detector simulation snapshot (figure 16(c)) the area of coverage of GAINS is smaller compared to their highly cost effective NaI(Tl) counterpart. But, being cost effective and having larger area of coverage does not warrant for the NaI(Tl) setup to be better.

6.1 Summary of main contributions

As seen in previous sections, the CsI detectors are not suitable to be used in a GAINS like setup. However, the detectors used in this study were not in top condition either. That being said, a good CsI detector has relatively low energy resolution compared to a good NaI(Tl) detector [15], hence it is fair to conclude that CsI detectors cannot be used in a GAINS-like setup.

The NaI(Tl) detector used in this study shows energy resolution between 6% to 8% for energies between 1 MeV and 1.4 MeV. The energy resolution of 7.23% at 1173.2 keV implies that the FWHM (ΔE) is 84.78 keV. This means that the NaI(Tl) detector can be used for measurements where the minimum energy difference between two consecutive energy peaks is $\geq$ 170 keV (1σ) within the energy range 1 MeV to 1.4 MeV for best results. According to various other studies, the NaI(Tl) detector has resolution between 4% and 6% for similar energies. This implies that the detector used in this study provides a fair and realistic evaluation as compared to the CsI detectors. Based on the resolution and efficiency alone the NaI(Tl) based GAINS-like setup is feasible depending on the scope of experiment. The NaI(Tl) based GAINS-like setup will sacrifice energy resolution for higher efficiency. However, whether to make the compromise or not will depend purely on the nature of the planned experiments.

6.2 Future Work

This research has focused on the energy dependent characteristics of CsI and NaI(Tl) based GAINS-like setups to check their viability to be used as or instead of the HPGe based GAINS spectrometer. Although insightful, this study does not cover the other important aspects of a detection system. These aspects include time based characteristics of the detection setup (ToF measurements) and the data acquisition algorithms used along with the spectrometer. Thus it is imperative to study these aspects before making an informed decision regarding the use of NaI(Tl) detectors in GAINS like configuration.

Acknowledgements

I came to the Netherlands to pursue my dream of being an experimental physicist. Although a difficult job for someone with my academic background, I do not regret the path I have chosen. I have met new people, interacted with many more. All these experiences have made me a better version of myself and I would like to take this opportunity to show gratitude to some individuals I appreciate and admire.

Dear Myroslav, from our first meeting in the basement lab I was in awe. Your speech entails your passion towards your work and your skills make it evident. The words you said, "Don't just know what you do, understand why you do it." will stay with me forever. I not only idolize you as a great experimental physicist but also as an amazing human being. And from the bottom of my heart, I am grateful to have the opportunity to work under your guidance.

Dear Nasser, its always a pleasure to be in your company. Whether its lunch, group meetings or being on the receiving end of your questions after presentations. I always have learned something while talking to you may it be academic or otherwise. Lastly, hearty congratulations once again on becoming the director of ESRIG. The institute sure has its best days lying ahead. I could only wish that I can get the opportunity to work under the power duo of you and Myroslav again.

Dear Muhsin, I am glad to have made your acquaintance. Even if my time spent in your company is limited, your stories of $\overline{\text{P}}$ANDA and international travels have kept me inspired to work in this field. Your enthusiasm and dedication even at this age is truly admirable.

Finally I would like to thank Jisk and Ali for their help not only with my thesis but also during our weekend culinary escapades. Even though I became your 'room mate' at the very end of my thesis, I enjoyed your company. Dear Ali, whether it be writing Code.C, arguing over academic topics or going on midnight bicycle rides, it was fun working and playing with you. Dear Jisk, thank you for teaching me to strive for elegance and perfection. Your cinephilic tendencies show off in your work and attitude. I wish we had more time as colleagues. I hope we all keep in touch.

In pursuit of my dreams, I have been staying away from home since 2012. Different cities, different country; it hardly made any difference. The only major impact was made by the people I met and experiences I shared. And I can confidently say that this thesis was one of the best experiences of my life.

"*Beim Menschen ist es wie beim Velo. Nur wenn er faehrt, kann er bequem die Balance halten.*"

— A. EINSTEIN

References

[1] Deleanu, D., et al. ”The gamma efficiency of the GAINS spectrometer.” Nuclear Instruments and Methods in Physics Research Section A: Accelerators, Spectrometers, Detectors and Associated Equipment 624.1 (2010): 130-136.

[2] Tsoulfanidis, Nicholas. Measurement and detection of radiation. CRC press, 2010.

[3] Borcea, Catalin, et al. ”Inelastic neutron scattering with GAINS at GELINA: An overview of the last decade.” EPJ Web of Conferences. Vol. 146. EDP Sciences, 2017.

[4] Agostinelli, Sea, et al. ”GEANT4—a simulation toolkit.” Nuclear instruments and methods in physics research section A: Accelerators, Spectrometers, Detectors and Associated Equipment 506.3 (2003): 250-303.

[5] Knoll, Glenn F. Radiation detection and measurement. John Wiley & Sons, 2010.

[6] Reilly, Doug, et al. Passive nondestructive assay of nuclear materials. No. NUREG/CR-5550; LA-UR-90-732. Nuclear Regulatory Commission, Washington, DC (United States). Office of Nuclear Regulatory Research; Los Alamos National Lab., NM (United States), 1991.

[7] Antcheva, Ilka, et al. ”ROOT—A C++ framework for petabyte data storage, statistical analysis and visualization.” Computer Physics Communications 180.12 (2009): 2499-2512.

[8] Akkurt, I., K. A. D. İ. R. Gunoglu, and S. S. Arda. ”Detection efficiency of NaI(Tl) detector in 511–1332 keV energy range.” Science and Technology of Nuclear Installations 2014 (2014).

[9] Allison, John, et al. ”Geant4 developments and applications.” IEEE Transactions on nuclear science 53.1 (2006): 270-278.

[10] Leo, William R. Techniques for nuclear and particle physics experiments: a how-to approach. Springer Science & Business Media, 2012.

[11] D’Agostini Herstad, Tatiana. Performance studies of data acquisition for the GAINS spectrometer at the GELINA accelerator facility. Diss. 2021.

[12] Negret, A., et al. ”The Limits of the GAINS Spectrometer.” Nuclear Data Sheets 119 (2014): 179-182.

[13] Perez-Andujar, A., and Leticia Pibida. ”Performance of CdTe, HPGe and NaI(Tl) detectors for radioactivity measurements.” Applied radiation and isotopes 60.1 (2004): 41-47.

[14] Tam, Hoang Duc, et al. ”Optimization of the Monte Carlo simulation model of NaI(Tl) detector by Geant4 code.” Applied Radiation and Isotopes 130 (2017): 75-79.

[15] Hawrami, Rastgo, et al. ”Growth and Evaluation of Improved CsI: Tl and NaI: Tl Scintillators.” Crystals 12.11 (2022): 1517.